A&A 433, 1047–1054 (2005)
DOI: 10.1051/0004-6361:20042019
© ESO 2005

Astronomy & Astrophysics

A survey for Fe 6.4 keV emission in young stellar objects in ρ Oph: The strong fluorescence from Elias 29

F. Favata[1], G. Micela[2], B. Silva[1], S. Sciortino[2], and M. Tsujimoto[3]

[1] Astrophysics Division – Research and Science Support Department of ESA, ESTEC, Postbus 299, 2200 AG Noordwijk, The Netherlands
e-mail: Fabio.Favata@rssd.esa.int
[2] INAF – Osservatorio Astronomico di Palermo, Piazza del Parlamento 1, 90134 Palermo, Italy
[3] Department of Astronomy and Astrophysics – Pennsylvania State University, 525 Davey Laboratory, University Park, PA 16802, USA

Received 15 September 2004 / Accepted 13 December 2004

Abstract. We report the results of a search for 6.4 keV Fe fluorescent emission in Young Stellar Objects (YSOs) with measured accretion luminosities in the ρ Oph cloud, using the existing *Chandra* and XMM-*Newton* observations of the region. A total of nine such YSOs have X-ray data with sufficiently high S/N for the 6.4 keV line to be potentially detected if present. A positive detection of the Fe 6.4 keV line is reported for one object, Elias 29, in both the XMM-*Newton* and the *Chandra* data. The 6.4 keV line is detected in Elias 29 both during quiescent and flaring emission, unlikely all previously reported detections of 6.4 keV Fe fluorescence in YSOs which were made during intense flaring. The observed equivalent width of the fluorescent line is large, $W_\alpha \simeq 160$ eV, ruling out fluorescence from diffuse circumstellar material. It is also larger than expected for simple reflection from a solar-composition photosphere or circumstellar disk, but it is compatible with being due to fluorescence from a centrally illuminated circumstellar disk. The X-ray spectrum of Elias 29 is also peculiar in terms of its high (ionized) Fe abundance, as evident from the very intense Fe XXV 6.7 keV line emission; we speculate on the possible mechanism leading to the observed high abundance.

Key words. stars: coronae – stars: formation – stars: individual: Elias 29 – stars: individual: ρ Oph

1. Introduction

The wealth of X-ray observations of star-forming regions carried out in the 1990's by ROSAT and ASCA have established young stars as bright X-ray sources throughout their evolution, from the Class I stage, where an accreting envelope is still present around the young star, throughout the Class III (or WTTS) stage, where very little circumstellar envelope remains and the star's photosphere is hardly distinguishable from that of a more mature similar object. Evidence for X-ray emission from true protostars (Class 0 objects) has come more recently, and it is still circumstantial.

While most YSOs are too far away for their X-ray emission to be studied with the current generation of X-ray high resolution spectrographs (with XMM-*Newton* and *Chandra*), using CCD-resolution spectra the X-ray emission from YSO's has been modeled as thermal emission from a hot plasma in coronal equilibrium, with higher characteristic temperatures than observed in older and less active stars. Due to their proximity to Earth the X-ray spectra from YSOs in both the Taurus and ρ Oph regions have been studied in some detail (e.g. the L1551 region in Taurus studied with XMM-*Newton*, Favata et al. 2003, the ρ Oph region studied with *Chandra*, Imanishi et al. 2002 and XMM-*Newton*, Ozawa et al. 2005), and in all cases the X-ray spectra were well fit with a hot thermal plasma. Embedded YSOs (Class I) and Classical T Tau stars (CTTS, or Class II) have higher characteristic X-ray temperatures than Weak-Line T Tau stars (WTTS, or Class III): in ρ Oph Ozawa et al. (2005) find characteristic X-ray temperatures ranging between 2.0 and 6.0 keV for Class I and Class II sources, while Class III sources have quiescent X-ray temperatures ranging between 0.3 and 2.5 keV. Best-fit coronal abundances are (in line with many coronal sources) rather low, with typical best fit values around 0.2–0.3 $Z_\odot$, with some cases (e.g. XZ Tau in L1551, Favata et al. 2003) showing very low abundances, $Z < 0.1\ Z_\odot$, where $Z_\odot$ is the solar photospheric abundance.

One notable deviation from a pure thermal X-ray spectrum has been detected in the X-ray emission of the YSO YLW16A in ρ Oph: during a large flare Imanishi et al. (2001) detected, in addition to the Fe XXV complex at 6.7 keV, a well visible 6.4 keV line which they attributed to fluorescence from "cold" (i.e. neutral, or in low ionization states) Fe. Such a line is produced when hard X-rays photo-ionize cold material close to

Article published by EDP Sciences and available at http://www.aanda.org or http://dx.doi.org/10.1051/0004-6361:20042019

Table 1. The sample of X-ray bright YSOs analyzed. The accretion luminosity reported is from Muzerolle et al. (1998).

Source name	Class	$\log L/L_\odot$	$\log L_{acc}/L_\odot$	XMM-*Newton*	*Chandra*
Elias 29	I	1.68[1]	1.25	y	y
WL 6	I	0.38[1]	−0.37	–	y
GSS 26	I	−0.15[1]	−0.57	y	gap
YLW 3B (SR 24S)	II	1.33[4]	0.34	y	–
Elias 24	II	0.23[2]	0.34	y	y
DoAr25	II	−0.08[3]	−1.34	y	–
V852 Oph (SR 22)	II	−0.08[4]	−1.34	y	–
VSSG 27	II	−0.96[3]	−0.86	–	y
VSSG 28 (GSS 39)	II	0.04[3]	−0.62	–	y

[1] From Muzerolle et al. (1998); [2] from Doppmann et al. (2003); [3] from Bontemps et al. (2001); [4] from Chen et al. (1995); [4] source unresolved from YLW 3B (see discussion in the text).

the X-ray source, and it is therefore an useful diagnostic tool of the geometry of the X-ray emitting source and its surroundings. The 6.4 keV fluorescent Fe line has been detected in a number of astrophysical sources, from massive stars to SNR to the Sun itself during flares, in which case the fluorescing material is the solar photosphere. In YSOs, in addition to the photosphere, also the circumstellar material could be responsible for the fluorescence, either from the circumstellar disk and its related accretion structures, or from more diffuse material.

Imanishi et al. (2001) do not discuss in detail the possible location of the fluorescing material, although, from the lack of a delay between appearance of the 6.7 keV and of the 6.4 keV lines they infer that the fluorescing material must be associated with the star and located at less than 20 AU from the X-ray source. The detection of Fe 6.4 keV fluorescent emission from YLW16A has remained unique, in the domain of cool stars, until the detection of Fe fluorescent emission in a number of flaring sources in the Orion cloud by Tsujimoto et al. (2005) (see also Tsujimoto et al. 2004). In all these cases the 6.4 keV fluorescent line was detected only during intense flares.

We present in this paper a survey for 6.4 keV fluorescent emission in X-ray bright YSOs in the ρ Oph cloud with measured accretion luminosity. The original aim of our work was to search for correlations between the characteristics of fluorescent emission and the accretion luminosity. Our search has resulted in the first detection of 6.4 keV fluorescent Fe emission in the quiescent emission from a YSO, Elias 29.

The present paper is structured as follows: Sect. 3 discusses the observations employed in the paper and their analysis, the sample of stars analyzed is described in Sect. 2, while the results are presented in Sect. 4. Elias 29 and its strong fluorescent X-ray emission are discussed in detail in Sect. 5, followed by the general discussion in Sect. 6. The conclusions are presented in Sect. 7.

2. The sample

Our starting sample consists of all the YSOs in the ρ Oph cloud which have measured accretion rates from Brγ luminosity in the work of Muzerolle et al. (1998). Being in the IR, the Brγ proxy of accretion luminosity is little affected by interstellar matter and allows to study also embedded sources.

From the parent sample we selected the sources which were visible as X-ray sources in at least one of the four X-ray observations listed in Table 2, and which had at least 500 net X-ray counts in the spectrum, allowing a reasonably detailed spectral analysis to be performed. The total number of YSOs satisfying this criterion is 9, of which 3 are Class I objects and 6 are class II. Given that some stars are present in both XMM-*Newton* and *Chandra* observations, a total of 12 spectra were analyzed.

The sample is listed in Table 1, showing the source name, its accretion and bolometric luminosity, and whether it was observed by *Chandra* or by XMM-*Newton*.

3. Observations and data analysis

The ρ Oph cloud has been observed by most X-ray imaging telescopes flown to date; in particular it has been the subject of two XMM-*Newton* and two *Chandra* deep observations, with different pointing directions (although with some overlap). While data from two *Chandra* observations and one XMM-*Newton* observations have already been published, we have, to be able to search for the 6.4 keV line in the individual spectra (and to ensure homogeneity), re-analyzed all 4 observations in a consistent way. The observations analyzed are listed in Table 2. No analysis of observation 1 has been published yet in the literature, while results from an analysis of observation 2 have been recently published by Ozawa et al. (2005). Results from observation 3 have been published by Imanishi et al. (2001) and Imanishi et al. (2003), who also have also published results from observation 4.

Both XMM-*Newton* observations have been processed using the same approach as described in Favata et al. (2003), to which the reader is refereed for details. Briefly, the observations have been fully reprocessed using the latest version of the SAS software (6.0), filtering out periods of high background ("proton flares"), and photon lists have been extracted for each source and for a relevant, nearby background region; spectra and light curves have then been produced.

Table 2. The four X-ray observations of the ρ Oph star-forming cloud analyzed in the present work.

N.	Mission	Date	Exp.	RA	Dec	PI
1	XMM-*Newton*	11-09-2000	50 ks	16:25:17.0	−24:16:48	F. Favata
2	XMM-*Newton*	19-02-2001	50 ks	16:27:26.0	−24:40:48	M. Watson
3	*Chandra*	14-04-2000	100 ks	16:27:18.1	−24:34:21	K. Koyama
4	*Chandra*	15-05-2000	100 ks	16:26:35.3	−24:23:12	M. Gagnè

Table 3. Results of spectral fitting to the X-ray spectra of the sample stars. All fits where performed with a one temperature absorbed APEC spectrum (fit results are given for a fit without a 6.4 keV line). Only Elias 29 showed evidence for the presence of 6.4 keV Fe fluorescence.

	XMM-*Newton*				*Chandra*			
Source	T_X (keV)	L_X erg s^{-1}	Z $Z_\odot$	χ^2	T_X (keV)	L_X erg s^{-1}	Z $Z_\odot$	χ^2
Elias 29	4.30 ± 0.5	1.1×10^{30}	1.06 ± 0.18	1.28	4.5 ± 0.8	7.3×10^{29}	0.60 ± 0.14	1.33
WL 6	–	–	–	–	1.2 ± 0.92	5.2×10^{27}	0.3	1.16
GSS 26	4.82 ± 1.1	6.7×10^{29}	0.40 ± 0.17	1.19	–	–	–	–
YLW 3B (SR 24S)	2.69 ± 0.33	6.4×10^{29}	0.16 ± 0.15	1.12	–	–	–	–
Elias 24	8.90 ± 5.2	8.6×10^{29}	0.3	0.70	4.0 ± 0.4	1.2×10^{30}	0.36 ± 0.15	1.24
DoAr25	5.24 ± 0.46	1.4×10^{31}	0.23 ± 0.07	0.97	–	–	–	–
V852 Oph	0.74 ± 0.15	1.1×10^{29}	0.3	0.74	–	–	–	–
VSSG 27	–	–	–	–	2.2 ± 0.4	5.5×10^{29}	0.3	1.24
VSSG 28	–	–	–	–	1.8 ± 1.3	1.5×10^{29}	0.3	1.05

Chandra observations have been obtained from the archive, and no further processing has been done on the cleaned photon lists; using CIAO threads, photon lists have been extracted for each source and for a relevant, nearby background region; spectra and light curves have then been produced.

For each of the X-ray bright sources (listed in Table 1) the spectra have been analyzed using XSPEC, and have been fit (in the energy band 1.0–8.0 keV) using single-temperature APEC models with varying global metal abundance including an absorbing column density modeled with a WABS model. In all cases the best-fit values are fully compatible with the values reported by Ozawa et al. (2005) for observation 2, and by Imanishi et al. (2001) and Imanishi et al. (2003) for observations 3 and 4. The presence of a 6.4 keV line was assessed by adding a Gaussian line to the spectrum, with initial energy $E = 6.4$ keV and fixed width (10 eV, the value expected from the width of the unresolved fluorescence lines), and determining (with the use of the F test) whether this resulted in a significant improvement in the fit.

4. Results

Table 3 shows the results of the spectral fitting performed on all the X-ray bright sources in ρ Oph. All sources could be adequately fit with a single temperature absorbed spectrum, whose parameters are reported in the Table.

Fluorescent line emission at 6.4 keV was detected, using the procedure described in Sect. 3, only in Elias 29; all other sources show no significant evidence of excess emission above the purely thermal spectrum. Two representative spectra and light curves (of the stars Elias 24 and DoAr25) are shown in Fig. 1.

4.1. Elias 29

Elias 29 is a well known luminous Class I YSO in the ρ Oph cloud. Using ISO observations Bontemps et al. (2001) determined its bolometric luminosity at $L_{\rm bol} = 26\ L_\odot$, making it the most luminous Class I source in ρ Oph. Muzerolle et al. (1998) have used the emission in the Brγ line to determine the object's accretion luminosity at $L_{\rm acc} = 15$–$18\ L_\odot$, making it the source with the highest accretion luminosity in their sample.

Given the large veiling, very little information is available on its characteristics; Doppmann et al. (2003) obtained high-resolution IR spectra, which are essentially featureless, indicating either a very large amount of veiling, or very fast rotation (or both).

Using sub-millimiter observations Boogert et al. (2002) have separated the contributions of the disk and of envelope surrounding the Elias 29 system, showing that the disk must be nearly face-on, with an inclination $i > 60$ deg ($i = 90$ deg being face-on). Their best-fitting disk model has an inner radius of 0.01 AU and an outer radius of 500 AU, and a mass $M = 0.012\ M_\odot$. Boogert et al. (2002) also argue that Elias 29 is a precursor of a Herbig AeBe star.

Using ISO and ground-based IR spectroscopic observations Ceccarelli et al. (2002a) derive the presence of a significant component, in the disk, of "super-heated" gas, which, they argue, may be (partly) due to the effects of high-energy (UV and X-ray) radiation from the central source.

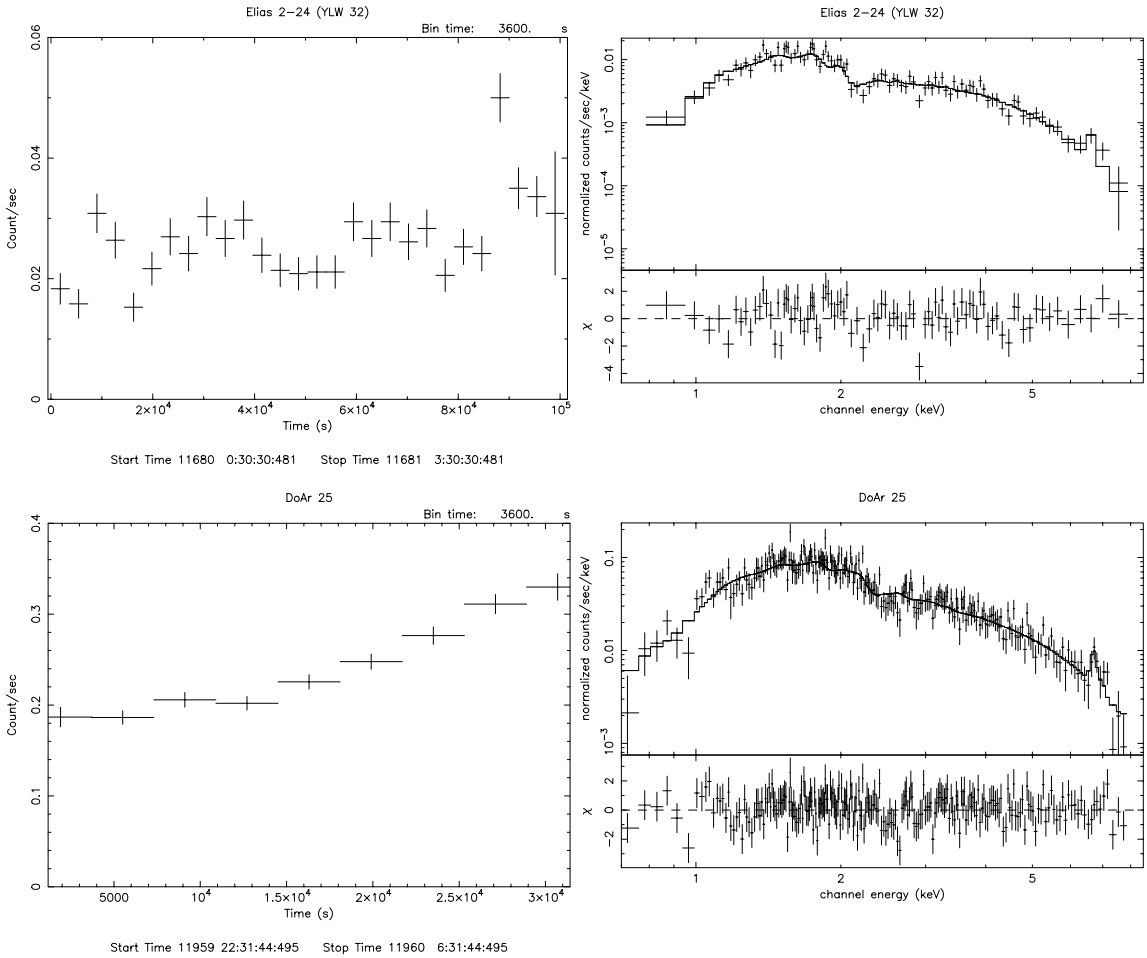

Fig. 1. *Top panels*: light curve and spectrum for the *Chandra* observation of Elias 24. *Bottom panels*: light curve and spectrum for the XMM-*Newton* observation of DoAr25.

Elias 29 has been observed in X-rays with ASCA, XMM-*Newton* and *Chandra*, and has been observed to flare repeatedly in X-rays (as common for YSOs), e.g. by Imanishi et al. (2001), who report flaring during the *Chandra* observation, and discuss the flares observed during the ASCA observations. The temperature of the plasma during the *Chandra* observations was, according to Imanishi et al. (2001), 4.3 keV in quiescence and 7.5 keV during the flare, with respective X-ray luminosities of 5.1×10^{30} and 2.0×10^{31} erg s^{-1}, with a fixed metal abundance $Z = 0.3\ Z_{\odot}$. The XMM-*Newton* observation of Elias 29 has been previously reported by Ozawa et al. (2005), who find coronal parameters consistent with our own ($T = 4.3$ keV, $Z = 1.0\ Z_{\odot}$).

5. The X-ray characteristics of Elias 29

The X-ray light curves (binned at 1 hr intervals) and spectra of Elias 29 are shown in Fig. 2 for both the XMM-*Newton* and *Chandra* observations. While a significant flare was present in the *Chandra* observation (as already reported by Imanishi et al. 2001), during the XMM-*Newton* observation the X-ray emission showed little variability, with the source at an essentially constant level. Both spectra are very hard, and with a very significant Fe 6.7 keV line emission, which, for the XMM-*Newton* EPIC pn spectrum, dominates even over the lower-energy continuum.

A joint spectral fit to the XMM-*Newton* pn, MOS1 and MOS2 data yields a best fit temperature $T = 4.3 \pm 0.5$ keV, a coronal abundance $Z = 1.1 \pm 0.2\ Z_{\odot}$, and a colum density $N(\mathrm{H}) = (4.8 \pm 0.3) \times 10^{22}$ cm^{-2}. The X-ray luminosity, in the 1–7 keV band, is 2.8×10^{30} erg s^{-1}. A fit to the *Chandra* spectrum (which has lower S/N than the XMM-*Newton* one) yelds a best fit temperature $T = 4.5 \pm 0.8$ keV, with a coronal abundance $Z = 0.60 \pm 0.15\ Z_{\odot}$. The column density is $N(\mathrm{H}) = (7.4 \pm 0.5) \times 10^{22}$ cm^{-2}. The spectral parameters of the X-ray spectrum of Elias 29 thus show little variation between the two observations.

While the high coronal temperature of Elias 29 is not exceptional, and is rather typical of Class I YSOs, the coronal metal abundance observed is very high (and the cause of such prominent 6.7 keV line emission); typical values for YSOs are around 0.2–0.3 $Z_{\odot}$ (e.g. in ρ Oph itself, Imanishi et al. 2001; Ozawa et al. 2005 or in Taurus; Favata et al. 2003), and no other X-ray bright YSO shows such high coronal metal abundance. While strong enhancements of the coronal metallicity have been observed during flares (e.g. Favata & Schmitt 1999 in Algol, or Tsuboi et al. 1998 in the YSO V773 Tau), the coronal metallicity of Elias 29 is consistently high across the

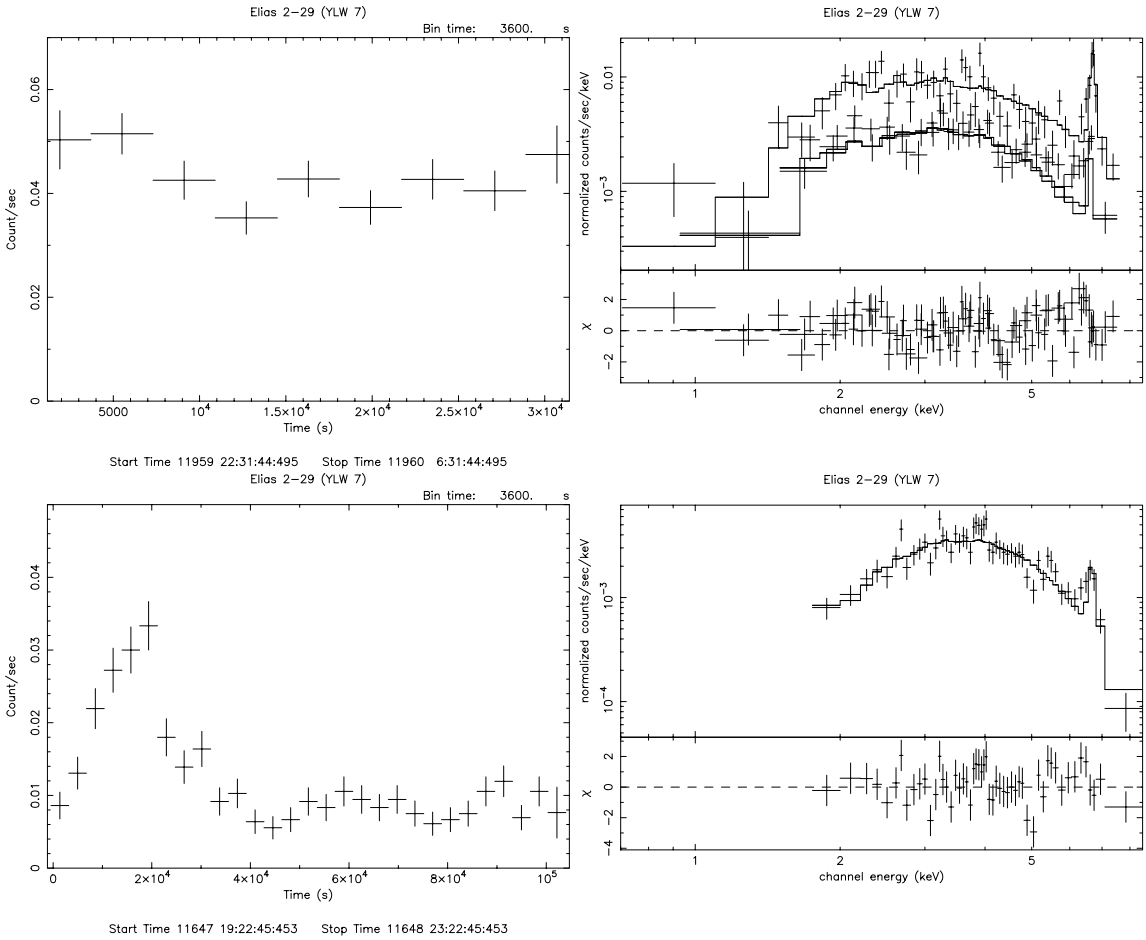

Fig. 2. X-ray light curves and spectra of Elias 29. The XMM-*Newton* light curve (pn only) and spectrum (for both the pn and MOS1 detectors) are shown in the upper panels, and the *Chandra* ones in the lower panels.

two observations, and, if anything, higher during the (quiescent) XMM-*Newton* observation than during the *Chandra* observation showing a flare.

5.1. Fluorescent Fe K emission in Elias 29

A significant excess of emission redward of the prominent Fe K complex at ≃6.7 keV, is visible in the *Chandra* spectrum of Elias 29 and (while less evident) is also well visible in the XMM-*Newton* spectrum. This excess emission occurs at the expected position of the 6.4 keV Fe fluorescent line; to determine whether indeed such emission is present in the X-ray spectrum of Elias 29 we have fit again the spectra with an additional Gaussian line component, which was constrained to be narrow (10 eV), while its wavelength and normalization were left free to vary. The other parameters (temperature, abundance and normalization of the thermal spectrum) were also left free to vary. The resulting fits are shown in Fig. 3, with the relevant parameters listed in Table 4. For the XMM-*Newton* data, for clarity, only the pn spectrum is shown in Fig. 3, although the fit has been performed on the joint pn+MOS spectra.

In both cases, as indicated in Table 4, the best-fit line energy agrees closely with the energy of the Fe fluorescent feature, with $E = 6.44 \pm 0.05$ keV for the *Chandra* spectrum and $E = 6.43 \pm 0.04$ for the joint XMM-*Newton* MOS+pn spectrum. The equivalent width of the line (W_α) is also similar across the two observations, at 150 eV and 120 eV for the *Chandra* and XMM-*Newton* spectra respectively. The F test applied to the χ^2 resulting from the fits with and without the additional Gaussian line shows that the feature is significant, with a null hypothesis probability of the line being the result of random fluctuation of 10% and 8% for the *Chandra* and XMM-*Newton* spectra respectively. In both cases, leaving the line width as a free parameter does not improve the fit significantly, and the fit converges onto essentially the same parameters, indicating that the feature present in the spectrum is compatible with being due to a narrow line.

To better determine the significance of the line, we also performed a joint fit to the XMM-*Newton* pn+MOS and *Chandra* ACIS spectra. The fit was performed (in the interval 4.0–8.0 keV) with the addition of a normalization constant (left free as a fit parameter) to allow for the difference in X-ray luminosity of the source between the XMM-*Newton* and *Chandra* observations. The χ^2 of the joint fit without the addition of the 6.4 keV line is 1.61 over 62 degrees of freedom (resulting in a low null hypothesis probability of 0.16%); the addition of the 6.4 keV line results in a much improved χ^2 of 1.21 over 60 degrees of freedom, corresponding to a much higher null

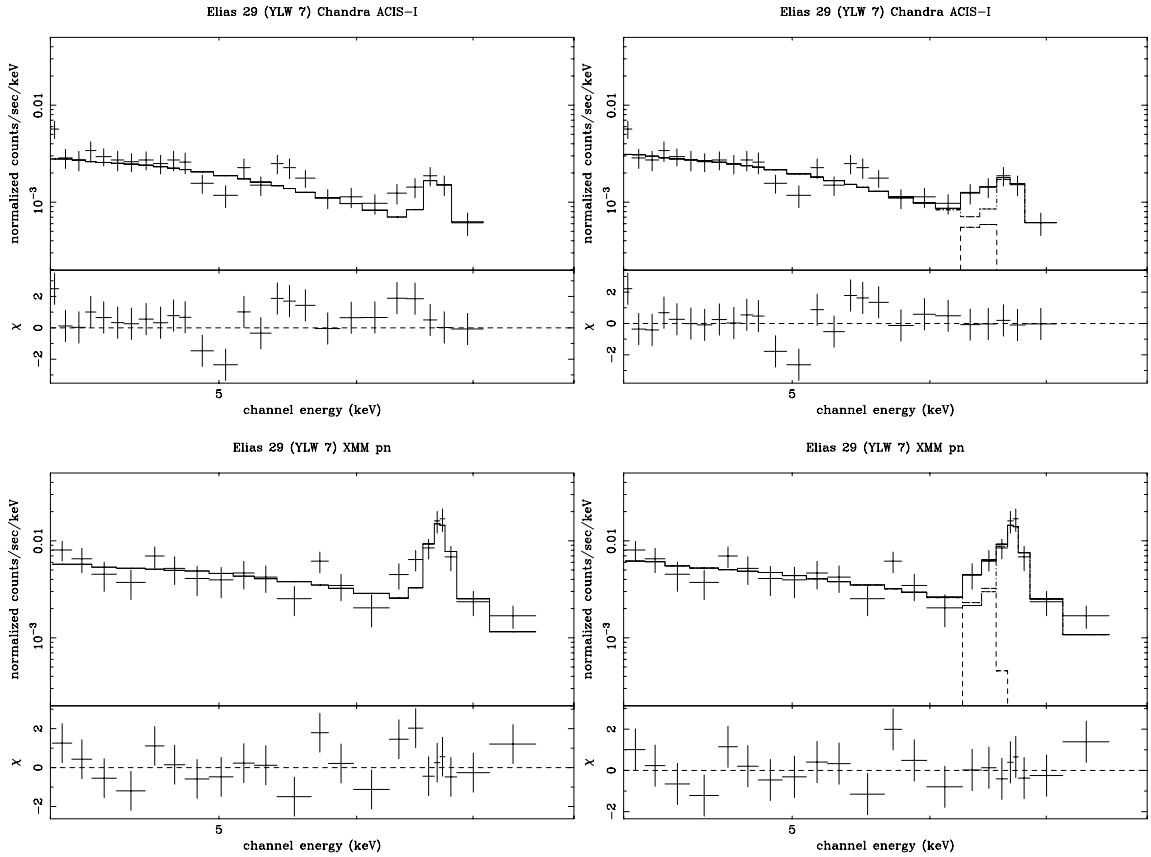

Fig. 3. The top spectra show the *Chandra* spectrum of Elias 29 in the 4.0–8.0 keV region, fit using an APEC thermal model (*left*) and with the addition of a narrow Gaussian component (*right*). The bottom spectra show the same for the XMM-*Newton* spectrum of Elias 29.

Table 4. Parameters of the 6.4 keV fluorescent line detected in the *Chandra* and XMM-*Newton* spectra of Elias 29. The line energy E is in keV, the line intensity in 10^{-6} photons cm^{-2} s^{-1} and the equivalent width W_α in eV. P is the probability that the detected line is due to a random fluctuation in the data.

Observation	E	I	W_α	P
ACIS-I	6.45 ± 0.05	(1.6 ± 1.3)	150	10%
pn+MOS	6.43 ± 0.04	(1.3 ± 1.0)	120	8%
ACIS-I+pn+MOS	6.43 ± 0.03	(1.8 ± 0.8)	160	<1%

hypothesis probability of 12%. This results in a very high significance of the line, better than 1% (again using the F test) and results in a 6.4 keV fluorescence line with an equivalent width of 160 eV, which we will adopt in the following as the average value of the fluorescence from Elias 29. We have also separately analyzed the *Chandra* flaring and non-flaring segments, but did not detect any difference regarding the presence of the fluorescent line emission. Finally, we verified that also the MEKAL and RAYMOND model produce similar results to the APEC model.

6. Discussion

Fluorescent emission from the Fe 6.4 keV line has thus far only been observed, for coronal sources, in intense flares from YSOs, with the initial detection in a flare in YLW16A by Imanishi et al. (2001), followed by the recent sample of YSOs in Orion (all in flaring state) by Tsujimoto et al. (2005) and Tsujimoto et al. (2004). Elias 29 is the first (and thus far only) coronal source for which fluorescent emission is clearly present in the quiescent state, i.e. in the absence of any significant flare. In fact, the presence of a moderate flare in the *Chandra* observation does not seem to influence the presence of the fluorescent emission, whose characteristics appear rather stable in time.

The intensity of the fluorescent emission is linked to both the amount of available photo-ionizing photons (for the Fe 6.4 keV line all the photons harder than the relevant photo-ionization edge, χ = 7.11 keV) and to the amount and geometry of the photo-ionized material.

In a simple formalism for the optically thin case, as discussed by Tsujimoto et al. (2005), the equivalent width of the 6.4 keV fluorescence line will be, under the assumption of a thermal spectrum with a temperature of a few keV illuminating the cold material,

$$W_\alpha[\mathrm{eV}] = 2.5\left(\frac{\Omega}{4\pi}\right)\left(\frac{N'_{\mathrm{H}}}{10^{22}\ \mathrm{cm}^{-2}}\right) \quad (1)$$

where Ω is the solid angle of fluorescing material illuminated by the thermal X-ray spectrum, and N'_{H} is the equivalent column density of the fluorescing material. In the case of Elias 29, with $W_\alpha \simeq 160$ eV,

$$N'_{\mathrm{H}} \simeq 6 \times 10^{23} \times \frac{4\pi}{\Omega}\ \mathrm{cm}^{-2}. \quad (2)$$

Given that the circumstellar column density toward the X-ray source determined spectroscopically is $N_{\rm H} = 4 \times 10^{22}$ cm^{-2}, this rules out (similarly to the Orion flaring sources discussed by Tsujimoto et al. 2005) fluorescence from diffuse circumstellar material. Also, the typical column density at which the ionizing photons are absorbed is $N_{\rm H} \simeq 10^{24}$ cm^{-2} (Bai 1979), so that the large equivalent width observed points to the presence of optically thick conditions.

Under optically thick conditions, the computation of the equivalent width of the fluorescence line requires a detailed radiative transfer treatment and the assumption of a well defined geometry for the absorbing material and for its illumination. George & Fabian (1991) have performed this computation for the case of an accretion disk illuminated either from above or from the central accreting source. In their treatment they assume illumination from an X-ray source with a power law spectrum, with photon indices Γ varying between 1.3 and 2.3. While the Elias 29 spectrum is well fit with a hot thermal spectrum, its continuum spectrum (ignoring the strong Fe 6.7 keV line, which however, having an energy below $\chi = 7.11$ keV, does not contribute to excite the fluorescence line) is equally well fit with an absorbed power law with $\Gamma = 2.6$, somewhat softer than the softer case studied by George & Fabian (1991), but still sufficiently close to allow a qualitative comparison. For the case of a disk illuminated from above, the George & Fabian (1991) computation shows that the equivalent width of the emitted fluorescent line varies roughly linearly with the photon index, and $W_\alpha \leq 100$ eV for $\Gamma > 2$. The emitted equivalent widths are somewhat larger (under the assumption of favorable viewing geometry) for the case of a centrally illuminated accretion disk, with $W_\alpha \leq 150$ eV for $\Gamma > 2$, compatible with the equivalent width measured in the Elias 29 spectrum.

The observed fluorescence line can thus be naturally explained as fluorescent emission from a centrally illuminated disk, seen face-on, a natural geometry if X-ray emission indeed is concentrated near the star. This implies that the disk is "bathed" in high-energy X-rays emitted by the star, thus supporting the hypothesis of Ceccarelli et al. (2002a) that the "hot" component they observe in IR in the disk is indeed heated by the stellar high-energy radiation. Ceccarelli et al. (2002b) have recently discovered calcite toward a protostar similar to Elias 29, and Chiavassa et al. (2005) report that calcite is also present toward Elias 29 itself. Given that calcite, under terrestrial conditions, requires the presence of liquid water to form Ceccarelli et al. (2002b) suggest that the calcite they observe may thus form on the surface of grains in the accretion disk, where water ice heated by the X-ray radiation may acquire an enhanced mobility. Again, the detection of fluorescent 6.4 keV radiation from Elias 29 shows that its accretion disk is indeed immersed in high-energy X-rays, and thus supports the above hypothesis for the formation of calcite.

The X-ray spectrum of Elias 29 is also peculiar in terms of its high coronal abundance, as visually shown by the strongly dominating Fe line in the spectrum. While the relationship between coronal and photospheric abundances is still far from clear (also largely due to the lack of photospheric abundance measurements for active stars), the coronal abundance has been observed to vary significantly during large flares, in a variety of stars (e.g. Algol, Favata & Schmitt 1999, EV Lac, Favata et al. 2001, the PMS V773 Tau, Tsuboi et al. 1998). In all cases, the abundance increases from the typical $Z \simeq 0.2$–$0.3\ Z_\odot$ "quiescent" value to $Z \simeq Z_\odot$. On the other hand, the X-ray spectrum of Elias 29 shows a high Fe abundance in its quiescent emission, with little if any influence from the small flare detected in the *Chandra* observation.

Other stars in our sample have comparable X-ray characteristic coronal temperatures, so that, in principle, a comparable number of photo-ionizing photons would be available to generate fluorescent emission. Yet, none of the other stars show any evidence for fluorescent emission, and they all show the usual low coronal abundance. While the information available on the characteristics of Elias 29 is limited, given its being highly embedded and its high degree of veiling, it is the most luminous source in the sample, both in terms of its intrinsic luminosity and of its accretion luminosity: at $L_{\rm acc} = 15$–$18\ L_\odot$ its accretion flux is more than one order of magnitude more luminous than any of the other stars discussed here.

While no correlation can be claimed on the basis of just one object showing a number of interesting characteristics (an unique intense Fe 6.4 keV fluorescence outside of flares and a very high accretion flux, together with a high metal abundance in the X-ray emitting plasma) it is tempting to speculate about the possible link among them, in terms of an emission driven X-ray mechanism (rather than a purely coronal one). The free fall speed for a normal (non-degenerate) star is too small for the infalling material to be heated at the ≃50 MK temperature observed in the X-ray spectrum of Elias 29, so that the simple shock heating at the accretion site which explains rather well the UV excess and the emission lines observed in the optical spectrum cannot be invoked in the present context. In the magnetospheric accretion scenarios normally invoked to explain the phenomenology of CTTS the plasma is channeled from the accretion disk onto the stellar surface in magnetic flux tubes, with one foot anchored on the stellar photosphere and the other onto the edge of the accretion disk. The currently most accredited mechanism for the heating of coronae is shearing of the footpoints of the loops induced by convective motions at the photosphere, where the loops are anchored. This mechanism would still operate on the stellar side of the magnetic flux tube funneling the accretion; on the accretion disk side, the Keplerian rotation of the disk would provide a natural shearing force on the different parts of the loop's footpoint at different distance from the star. Thus, the accreting plasma in the magnetic flux tube funneling the accretion would be subject to the same heating mechanisms as the plasma in normal coronal loops, and would efficiently emit X-rays. The key difference would be the continuous flow of fresh material in the flux tube, similarly to what happens during the rise phase of a flare due to chromospheric evaporation. This would naturally justify the high metal abundance for the X-ray emitting plasma in Elias 29, similarly to the short-term increase in coronal metallicity observed during stellar flares, in which the coronal abundance (likely due to the rapid influx of chromospheric and photospheric material into the magnetic loop) briefly increases to photospheric values. In the case of flares, once the flow is stopped, the fractionation mechanism rapidly brings the coronal abundance back to its

pre-flare value; in the mechanism for the X-ray emission from Elias 29 speculated here, the sustained flow from the accretion disk into the magnetic flux tube would maintain the high abundance in the X-ray emitting plasma.

7. Conclusions

Our survey for Fe 6.4 keV fluorescent emission in YSOs with measured accretion luminosity in ρ Oph has yielded a positive detection in the Class I YSO Elias 29, for which the 6.4 keV line is detected in both the XMM-*Newton* and the *Chandra* spectra. While in previous detections of Fe 6.4 keV emission in YSOs the sources are always in a flaring state, we detect the 6.4 keV emission in Elias 29 also while its thermal X-ray emission shows no temporal variability. The thermal X-ray spectrum of Elias 29 has an average characteristics temperature of $\simeq$4.6 keV, high but not exceptional among YSOs. Its Fe abundance is on the other hand very high, with $Z = 1.1\,Z_{\odot}$ in the XMM-*Newton* observation.

The equivalent width of the 6.4 keV line observed in Elias 29 is large, with an average $W_{\alpha} = 160$ eV. The strength of the line rules out reflection or transmission from diffuse circumstellar material, and requires an optically thick reflector. However, reflection from a photosphere or circumstellar disk of solar photospheric composition illuminated from above cannot produce, given the X-ray spectrum of Elias 29, a line of this strength. The observed equivalent width can however be explained in a scenario in which the circumstellar disk is illuminated by a centrally placed X-ray source, if the disk is observed face-on. This scenario naturally explains the observed fluorescent emission in Elias 29 (in which IR observations also show the disk to have a large inclination, $i > 60$ deg, compatible with its being face-on) and may simply explain the paucity of YSOs in which 6.4 keV has thus far been observed as a purely geometric effect, its detection requiring observation of a (low-probability) face-on system.

The high abundance of the X-ray emitting plasma of Elias 29 could also be naturally explained if the plasma is confined, rather than in "classic" coronal loops, in magnetic flux tubes with one foot on the star and the other on the accretion disk (as expected in the magnetospheric model of accretion). In this case, material would continuously flow within the tube, and whatever chemical fractionation mechanism is responsible for the low abundances observed in "coronal" YSOs would be counterbalanced by the continuous flow of fresh, undepleted material in the corona.

Acknowledgements. We wish to thank C. Ceccarelli for the useful discussions and for providing us with material prior to publication. GM, SS acknowledge the partial support of ASI and MURST. This paper makes use of observations obtained with XMM-*Newton*, an ESA science mission with instruments and contributions directly funded by ESA Member States and the USA (NASA). MT is financially supported by the Japan Society for the Promotion of Science.

References

Bai, T. 1979, Sol. Phys., 62, 113
Bontemps, S., André, P., Kaas, A. A., et al. 2001, A&A, 372, 173
Boogert, A. C. A., Hogerheijde, M. R., Ceccarelli, C., et al. 2002, ApJ, 570, 708
Ceccarelli, C., Boogert, A. C. A., Tielens, A. G. G. M., et al. 2002a, A&A, 395, 863
Ceccarelli, C., Caux, E., Tielens, A. G. G. M., et al. 2002b, A&A, 395, L29
Chen, H., Myers, P. C., Ladd, E. F., & Wood, D. O. S. 1995, ApJ, 445, 377
Chiavassa, A., Ceccarelli, C., Tielens, X., Caux, E., & Maret, S. 2005, A&A, 432, 547
Doppmann, G. W., Jaffe, D. T., & White, R. J. 2003, AJ, 126, 3043
Favata, F., & Schmitt, J. H. M. M. 1999, A&A, 350, 900
Favata, F., Micela, G., Reale, F., & Sciortino, S. 2001, A&A, 375, 485
Favata, F., Giardino, G., Micela, G., Sciortino, S., & Damiani, F. 2003, A&A, 403, 187
George, I. M., & Fabian, A. C. 1991, MNRAS, 249, 352
Imanishi, K., Koyama, K., & Tsuboi, Y. 2001, ApJ, 557, 747
Imanishi, K., Tsujimoto, M., & Koyama, K. 2002, ApJ, 572, 300
Imanishi, K., Nakajima, H., Tsujimoto, M., Koyama, K., & Tsuboi, Y. 2003, Publ. Astr. Soc. Japan, 55, 653
Muzerolle, J., Hartmann, L., & Calvet, N. 1998, AJ, 116, 2965
Ozawa, H., Grosso, N., & Montmerle, T. 2005, A&A, in press
Tsuboi, Y., Koyama, K., Murakami, H., et al. 1998, ApJ, 503, 894
Tsujimoto, M., Feigelson, E., Grosso, N., et al. 2004, in Cool Stars, Stellar Systems and the Sun, ed. F. Favata, & G. Hussain, ESA-SP 560, in press
Tsujimoto, M., Feigelson, E., Grosso, N., et al. 2005, ApJS, in press